International Journal of Humanoid Robotics
Vol. 9, No. 4 (2012) 1250027 (24 pages)

DOI: 10.1142/S0219843612500272

World Scientific
www.worldscientific.com

THE DESIGN OF THE iCub HUMANOID ROBOT

ALBERTO PARMIGGIANI[*,‖], MARCO MAGGIALI[*,**], LORENZO NATALE[*,††], FRANCESCO NORI[*,‡‡], ALEXANDER SCHMITZ[*,§§], NIKOS TSAGARAKIS[†,¶¶], JOSÉ SANTOS VICTOR[‡,‖‖], FRANCESCO BECCHI[§,***], GIULIO SANDINI[*,¶,†††] and GIORGIO METTA[*,¶,‡‡‡]

[*]*Robotics Brain and Cognitive Sciences Department, Istituto Italiano di Tecnologia, Via Morego 30, 16163 Genova, Italy*

[†]*Advanced Robotics Department, Istituto Italiano di Tecnologia, Via Morego 30, 16163 Genova, Italy*

[‡]*Institute of Systems and Robotics, Instituto Superior Técnico, Av. Rovisco Pais, 1049-001 Lisboa, Portugal*

[§]*Telerobot OCEM s.r.l., Via Semini 28C 16163 Genova, Italy*

[¶]*DIST, University of Genoa, Viale Causa, 13 16145 Genova, Italy*

[‖]*alberto.parmiggiani@iit.it*
[**]*marco.maggiali@iit.it*
[††]*lorenzo.natale@iit.it*
[‡‡]*francesco.nori@iit.it*
[§§]*alexander.schmitz@iit.it*
[¶¶]*nikos.tsagarkis@iit.it*
[‖‖]*jasv@isr.ist.utl.pt*
[***]*becchi@telerobot.it*
[†††]*giulio.sandini@iit.it*
[‡‡‡]*giorgio.metta@iit.it*

Received 2 August 2010
Accepted 1 July 2012
Published 6 November 2012

This article describes the hardware design of the iCub humanoid robot. The iCub is an open-source humanoid robotic platform designed explicitly to support research in embodied cognition. This paper covers the mechanical and electronic design of the first release of the robot. A series upgrades developed for the second version of the robot (iCub2), which are aimed at the improvement of the mechanical and sensing performance, are also described.

Keywords: Humanoid robotics; open source; cognitive system.

1. Introduction

In recent years there has been a growing worldwide attention to the development of humanoid robots. Although these robots are intended for real world applications most of them are at the moment at the status of research prototypes to address the problems of mobility,[1,2] entertainment[3–5] and service robotics[6–8] to cite a few. Humanoid robots are also often used as a model to study human behavior.[9–12] The iCub (shown in Fig. 1) can be considered as a member of the latter category.

2. RobotCub: Open Source Robotics

Open source robotics, especially in its recent evolution, can be given two different flavors covering respectively the software components required to operate a robot platform (or a set of robot platforms) or the mechanical hardware. Examples of the first category are Orocos,[13] OpenRTM[a] and the Robot Operating System (ROS)[14] which is a recent attempt of standardizing middleware for mobile robotics. One slightly older example of the latter is the Japanese open source robot Pino.[15] There is also a notable activity in the creation of open source electronic design and this is summarized for example in the activities of the OpenCores.[b]

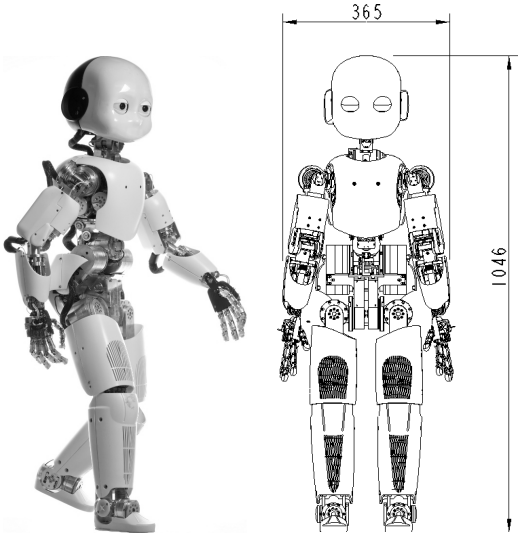

(a) (b)

Fig. 1. The iCub. The figure shows a photograph of the iCub robot (a). The overall robot dimensions are shown in (b).

[a] *http://www.openrtm.org/.*
[b] *http://www.opencores.org.*

The iCub[c] is one of the results of the RobotCub project, a EU-funded endeavor to create a common platform for researchers interested in embodied artificial cognitive systems.[16] Here the RobotCub project took a strong stance towards open source by releasing everything of the Consortium work as GPL, FDL or LGPL: this includes the mechanical and electronics design together with the software infrastructure of the iCub. The software infrastructure is based on an open source middleware called YARP which can compile cleanly on a number of operating systems (supported on Linux, Windows and MacOS) using a well-established set of tools.[17]

For the design of the electronics and mechanics, we were forced to use proprietary CAD tools, due to the absence of open source professional counterparts. This is an unfortunate situation, but there is no practical alternative at the moment. Free of charge, viewers are available for all file formats employed by the project. This does not prevent however the copy or reproduction of the iCub components since 2D drawings or Gerber files suffice in manufacturing parts and printed circuit boards (PCBs).

In supporting our open source stance, considerable effort was devoted to create an appropriate documentation of the robot. The current iCub documentation covers nearly all aspects of the robot design, from the mechanical hardware to the operating software. For RobotCub, it was decided to release all the CAD files under the GPL.[d] The associated documentation was also licensed under the GPL.[e] The YARP middleware is licensed either as GPL or LGPL.

3. Mechanical Design of the iCub

This section describes the details of the mechanical design of the iCub robot. In its final release at the end of the RobotCub project, the iCub is approximately 1 m tall (see Fig. 1(b)), has 53 active degrees of freedom (DOF) and has a mass of approximately 24 kg.

3.1. *Design specifications*

The initial specifications for the design of the robot aimed at replicating the size of a three-year-old child.[18] In particular, it was required that the robot be capable of crawling on all fours and possess fine manipulation abilities. For a motivation of why these features are important, the interested reader is referred to Metta *et al.*[16] The initial dimensions, kinematic layout and ranges of movement were drafted by considering biomechanical models and anthropometric tables.[16,19] Rigid body simulations allowed to determine which were the crucial kinematic features of the human body to be replicated in order to perform the set of desired tasks and motions.[16,20] These simulations also provided joint torques requirements: these data were then

[c] *http://www.icub.org.*

[d] The CAD models of the robot are available at: *http://robotcub.svn.sourceforge.net/viewvc/robotcub/trunk/iCubPlatform1.1/.*

[e] The documentation of the robot can be consulted at: *http://eris.liralab.it/wiki/Manual.*

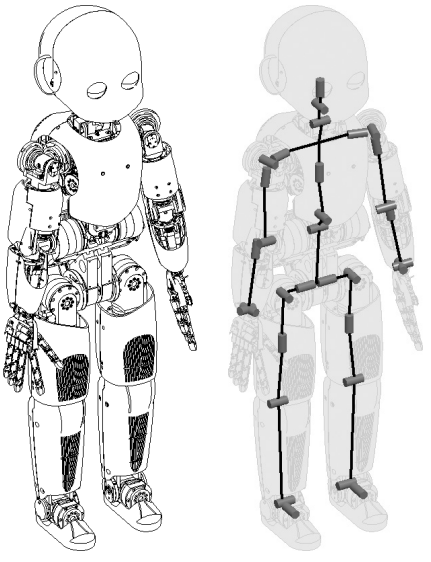

(a) (b)

Fig. 2. The iCub kinematic structure. The figure shows a CAD representation of the iCub (a) and of its kinematic structure (b). For visual clarity the representation of the eyes and hand joints has been omitted.

used as a baseline for the selection of the robot's actuators. The final kinematic structure of the robot is shown in Fig. 2(b). The iCub kinematic structure has several peculiar features which are rarely found in humanoid robots. The waist features a three DOF torso which considerably increases the robot's mobility. Moreover the three DOF shoulder joint is constructed such that its three axes of rotation always intersect at a single point. The list of the main DOF of the iCub robot is listed in Table 1; for more detailed information the reader shall refer to the official iCub documentation.[f]

3.2. *Actuators*

To match the aforementioned torque requirements several actuator technologies were considered.[21,22] Among the various alternatives rotary electric motors coupled with speed reducers were preferred because of their higher robustness and reliability. In total three modular motor groups with different characteristics were developed; this allowed their reuse throughout the main joints of the robot. All of them comprise a Kollmorgen-DanaherMotion RBE type brushless frameless motor[g] and a CSD frameless harmonic drive flat speed reducer[h] (see Fig. 3). Brushless motors have a

[f] *http://eris.liralab.it/wiki/ICubForwardKinematics.*
[g] Kollmorgen DanaherMotion product website:
http://www.kollmorgen- seidel.de/website/com/eng/download/document/200512291032290.
[h] HarmonicDrive product website:
http://www.harmonicdrive.net/media/support/catalogs/pdf/csd-shd-catalog.pdf.

Table 1. The joints of the iCub. The table lists the main joints of the iCub robot and their respective range of motion.

	Degree of freedom	Range of motion [deg]	
shoulder	pitch	−95	+10
	roll	0	+160
	yaw	−37	+80
elbow	flexion/extension	+5	+105
	pronation/supination	−30	+30
wrist	flexion/extension	−90	+90
	abduction/adduction	−90	+90
waist	roll	−90	−90
	pitch	−10	+90
	yaw	−60	+60
hip	flexion/extension	−120	+45
	abduction/adduction	−30	+45
	rotation	−90	+30
knee	flexion/extension	0	+130
ankle	flexion/extension	−60	+70
	abduction/adduction	−25	+25
neck	pan	−90	+90
	tilt	−80	+90
	roll	−45	+45

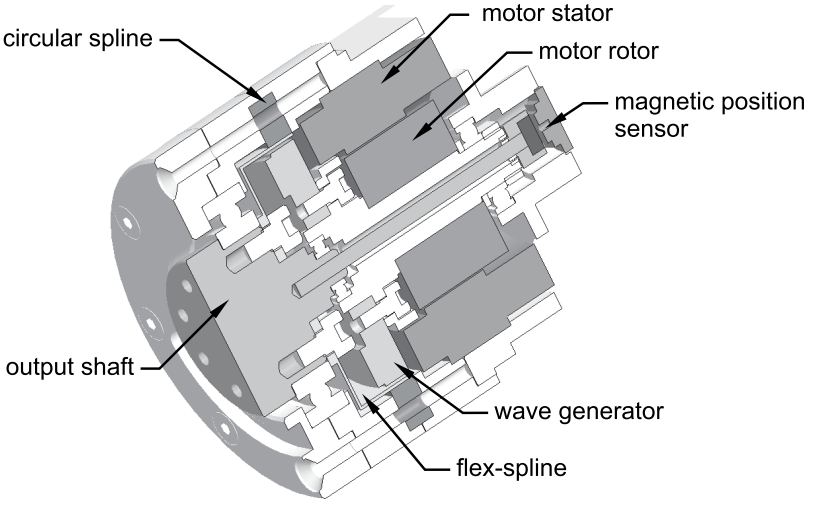

Fig. 3. Motor group cross section. The figure shows a cross section of a iCub motor group. The harmonic drive and Kollmorgen brushless motor are clearly visible.

very good power density and generally outperform conventional brushed DC motors. Harmonic drive speed reducers are very light, have practically no backlash, and allow very high reduction ratios in small spaces. The use of frameless components allows further optimization of space and to avoid the unnecessary weight of the housings. The characteristics of the actuator modules are the following:

- the high power motor group: capable of delivering 40 Nm of torque, it is based on the RBE 01211 motor and a CSD-17-100-2A harmonic drive, and has, roughly, a diameter of 60 mm and a length of 50 mm.
- the medium power motor group: capable of delivering 20 Nm of torque, it is based on the RBE 01210 motor and a CSD-14-100-2A harmonic drive, and has, roughly, a diameter of 50 mm and a length of 50 mm.
- the low-power motor: capable of delivering up to 11 Nm it is based on the RBE 00513 motor and a CSD-14-100-2A harmonic drive and has, approximately a diameter of 40 mm and a length of 82 mm.

3.3. *Cable drives*

In the design of the robot cable drive transmissions are widely employed. Cable transmissions can be used to efficiently transmit power from an actuator to a driven link whose range of rotation is limited. Cable drives allow the transmission of power between bodies rotating along different axes with driven pulleys, stepped pulleys, pinions and idle pulleys. Whenever space is limited they are a good alternative to geared transmission. Despite this kind of transmission generally has a lower mechanical stiffness than gears, if designed properly, it generally allows to obtain higher efficiencies. Moreover cable drives can be used to construct epicyclic transmission mechanisms similar to the one introduced by Salisbury *et al.*[23,24] and refined by Townsend.[25] In normal "serial" manipulators all the motors and speed reduction units are mounted directly on the joints, thus increasing the inertial loads on the motors. Instead by using coupled cable transmission the joints can be driven remotely: motors can thus be mounted in the proximity of the joint rather than on the joint itself. A mechanism of this kind has several advantages among which are a more compact size and lower weights and inertias if compared to standard serial designs. Another advantage is that this kind of transmission generally allows to obtain larger workspaces. However it is generally affected by some drawbacks such as higher mechanical complexity (therefore higher manufacturing costs and longer assembly time) and less intrinsic robustness. Examples of the implementation of cable drives can be found in the shoulder, elbow, torso, hip and ankle joints.

Let us consider, for illustrative purposes, the assembly of the two stage shoulder roll joint, represented in Figs. 4 and 5. The output shaft of the motor block comprises a pulley that is connected to an idle pulley, that is coaxial with the main motor group of the shoulder joint. This connection is obtained with two high resistance steel

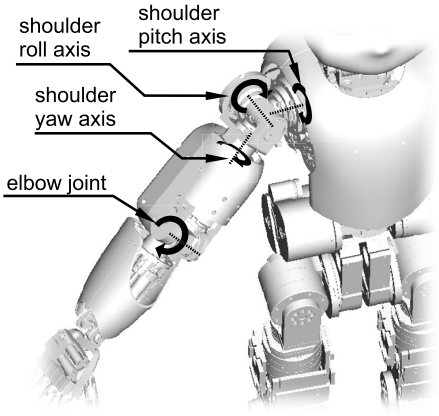

Fig. 4. The iCub arm. The figure represents a CAD view of the arm of the iCub and its three DOF shoulder joint and one DOF elbow joint.

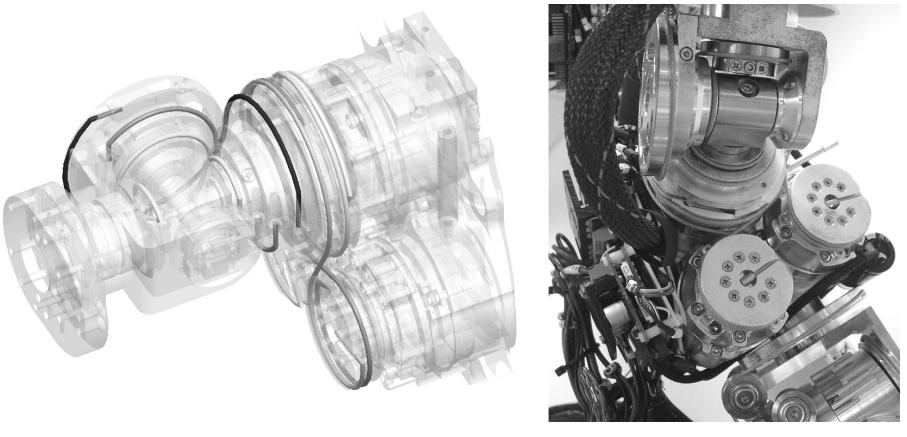

(a) (b)

Fig. 5. The shoulder joint. The figure shows a CAD view of the shoulder joint mechanism with a highlight of the cable transmission system (a). The figure also shows a photo of a bottom view of the shoulder joint (b).

cables (1.5 mm cross sectional diameter), manufactured by Carlstahl[i] and represented in Fig. 5(a). Because cables can only transmit forces through tension, two of them are always necessary to obtain forward and backward motion. Two other cables (also represented in Fig. 5(a)) connect the idle pulley to the output assembly with pulleys that intersect at a 90° angle, thus constituting the second stage of the transmission. Since the two cables cannot be wound on the same cylindrical surface

[i]Manufacturer's website: *http://www.carlstahl.de/*.

(as suggested by Townsend[24]), a stepped pulley is employed to allow the correct cable routing.

3.4. *Materials selection*

The total weight design specification was particularly difficult: special care had to be taken in the design of structural elements to avoid adding mass. For what concerns the materials, the majority of the parts of the robot were fabricated with the Al6082 aluminum alloy. With its ultimate tensile strength (UTS) of 310 MPa and roughly the typical density of aluminum 2700 kg/m^3, Al6082 is among the best materials in the 6000 alloy series.[j] For these reasons it was widely employed for all the parts that did not require particular resistance characteristics. Another material that has been employed the id Al7075 aerospace aluminum alloy because of its excellent strength to weight ratio. The use of zinc as the primary alloying element results in a strong material, with good fatigue strength and average machinability. The density of Al7075 has a density of 2810 kg/m^3 which is slightly higher than normal aluminum; its UTS of 524 MPa[k] is comparable with that of medium quality steels and make it one of the toughest types of aluminum alloys currently available. Components with more demanding mechanical properties were therefore manufactured with this material. Finally, highly stressed parts (such as joint shafts) were obtained from the high resistance stainless steel 39NiCrMo3. This material, known in the AISI standard as AISI9840, is a nickel−chromium−molybdenum steel, that exhibits a good combination of strength, fatigue resistance, toughness and wear resistance. Its UTS is high, around 1.2 GPa.[l]

3.5. *The arm and elbow assemblies*

The iCub arm has two joints: a three DOF proximal "shoulder" joint and a rotational distal "elbow" joint (see Fig. 4). The shoulder movements are obtained by means of a cable driven epicyclic transmission of the kind described in Sec. 3.3 which is shown in Fig. 5(a). The three motors driving the shoulder are housed in the upper-torso aluminum frame. The first motor actuates directly the shoulder pitch joint whereas the second and third motors actuate two pulleys that are coaxial with the first motor. These pulleys have slightly different primitive diameters thus producing a transmission reduction equal to the ratio of their diameters. The pulley motion is then transmitted to the shoulder roll and yaw joints through a second set of idle pulleys (see Figs. 5(a) and 5(b)). As a result the shoulder joint has its three axes of rotation intersecting at a single point (which is a typical characteristic of robotic wrist mechanisms) thus allowing "quasi"-spherical movements.

[j] Al6082 Matweb datasheet:
http://www.matweb.com/search/datasheet_print.aspx?matguid=fad29be6e64d4e95a241690f1f6e1eb7.
[k] Al7075 Matweb datasheet: *http://www.matweb.com/search/datasheet_print.aspx?matguid=9852e9cdc3d4466ea9f111f3f0025c7d.*
[l] 39NiCrMo3 Matweb datasheet:
http://www.matweb.com/search/datasheet_print.aspx?matguid=697130f21da64542a68bf61911f2f495.

This unconventional construction introduces kinematic couplings between the different motions. Because of this coupling, however, the relation between the displacements and the torques at motor and joint level is not straightforward. The technique outlined by Tsai for robotic wrist mechanisms[26] is particularly convenient for the analysis of complex epicyclic transmissions and allows to derive these relations for the iCub shoulder mechanism.[27]

The one DOF elbow joint is rather simple in its design. The output link is driven through a pulley system which transmits the power from the motor group. The motor is housed at the center of the assembly oriented 90° with respect to the axis of rotation of the elbow. A six-axis force−torque sensor is mounted at the interface between the shoulder and elbow assembly.

3.6. *The forearm and hand groups*

The hand of the iCub has been designed to enable dexterous manipulation as this capability is crucial for natural grasping behaviors (which are in turn fundamental for our research in cognitive systems). The hand of the iCub has 19 joints but is driven by only nine motors: this implies that group of joints are under-actuated and their movement is obtained with mechanical couplings. Similarly to the human body most of the hand actuation is in the forearm subsection. In particular, seven out of the nine motors driving the hand joints are placed in the forearm assembly. Given the limited amount of space available 0.36 to 2.57 W brushed DC electric motors were employed. These electric motors are coupled to multistage planetary speed reducers (whose reduction ratios vary from 159:1 to 256:1) to obtain the desired torques. The output shaft of the motors is connected to capstans which wind and unwind the steel cables that drive the phalanges movements.

The tendon arrangement is extremely critical; therefore the cable routing had to be done with extreme care and neatly organized according to specified guidelines[m] (see Fig. 6(b)). Moreover each tendon has to be tensioned properly: this was achieved by inserting double screwed tensioners along each cable.

The wrist is driven by a differential transmission mechanism of the type described in Sec. 3.3. On the other hand the flexing of the fingers is directly driven by the motors while their extension relies on a spring return mechanism, thus reducing the overall complexity of the device. The motion of the proximal phalanx and medial and distal phalanges are independent for the thumb, the index and the middle finger. The ring and small finger motions are coupled and driven by a single motor. Finally two motors, placed directly inside the hand assembly, are used for adduction/abduction movements of the thumb and of the index, ring and small fingers. The position of each phalanx is sensed by 17 small custom magnetic position sensors.

[m]The documentation can be consulted at: *http://robotcub.svn.sf.net/viewvc/robotcub/trunk/iCubPlatform/doc/assembly/tendonsHand2007.pdf.*

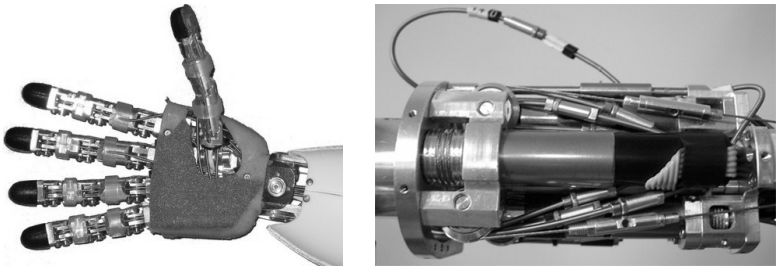

(a) (b)

Fig. 6. The right forearm and hand of the iCub. The figure shows a photo of the right hand of the iCub (a) and of the right forearm (b). The motor-capstan arrangement and the cable tensioning devices, described in the main text can clearly be seen in (b).

The overall size of the hand is extremely compact with its 50 mm in length, 60 mm in width and 25 mm in thickness, making it one of the smallest and most dexterous of its kind. The design of the iCub hand has been addressed in greater detail in a recent paper by Schmitz *et al.*[28] to which the reader shall refer for additional informations.

3.7. *The lower body and the torso*

The preliminary phases of the design process described in Sec. 3.1 suggested that for effective crawling a two DOF waist/torso mechanism is adequate. However, a three DOF waist was preferred to increase the range and flexibility of motions of the upper body. As a result the robot can lean, sideways, forwards and backwards, and rotate its body along its sagittal axis.

The torso mechanism is also based on the differential epicyclic transmission described in Sec. 3.3. In this case however the two base motors drive a third motor group, whose axis is orthogonal to the previous motors. The first two motors actuate jointly the pitch and roll axes whereas the third motor drives the yaw joint. The torso subassembly is shown in Fig. 7.

Since, for the leg space and size constraints were not particularly critical, the lower body was designed with a more standard "serial" configuration. The legs of the iCub comprise a three DOF joint at the hip. In this joint the first DOF is driven remotely by means of a cable drive actuated by a motor which is located in the lower torso assembly (see Fig. 8(a)). The leg includes a one DOF knee joint, actuated by the knee flexion/extension motor, and a two DOF ankle (see Fig. 8(b)). Each ankle is actuated by a frameless brushless motor housed in the lower leg segments which drives the flexion/extension movement and by a smaller motor group for the abduction/adduction movement which is placed directly on the foot.

3.8. *The head*

The primary function of the head assembly is to move cameras in order to quickly observe the environment. Two small video cameras are therefore available on the

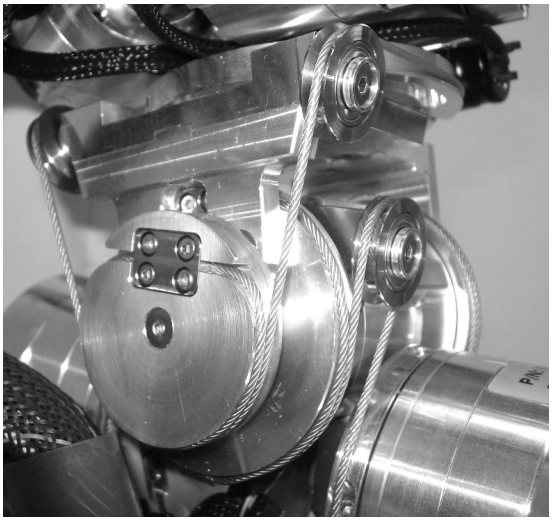

Fig. 7. The torso of the iCub. The figure shows a photo of the 3DOF torso mechanism and in particular the construction of the differential cable drive transmission.

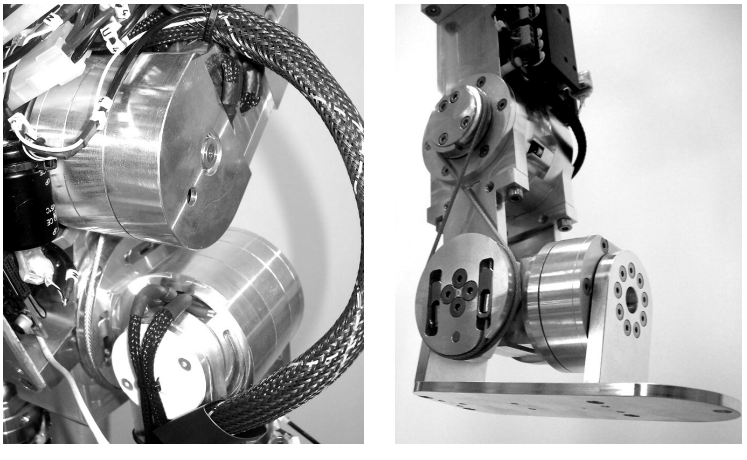

(a) (b)

Fig. 8. Details of the legs. The figure shows detail photographs of the legs of the iCub robot. The first two axes of the 3DOF hip are shown in (a). The 2DOF ankle is shown in (b).

iCub eyes (contained entirely inside the eyeballs). These cameras are moved by a three DOF eyes mechanism which allows both tracking and vergence behaviors. The compact neck mechanism has three additional DOF arranged in a serial pitch, roll and yaw configuration (see Fig. 1(c)). The three neck joints are driven by brushed DC motors coupled with low backlash Gysin speed reducers, to avoid problems when performing visual tasks. The eyes movements are also achieved with three DC

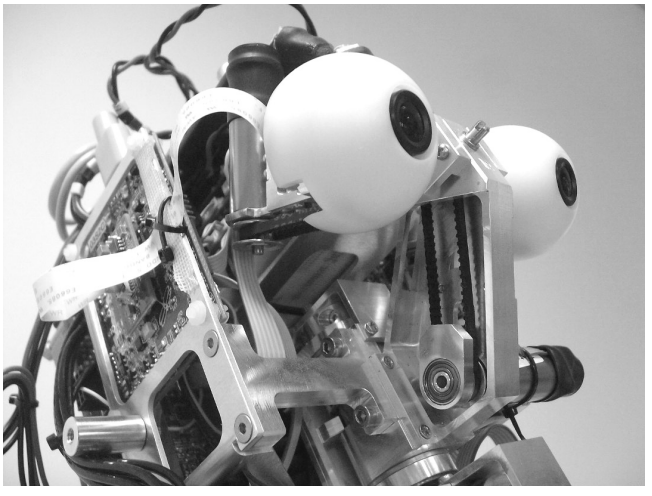

Fig. 9. Eyes mechanism. The figure shows a photo of the eyes mechanism; in particular the toothed belt transmissions of the eyes tilt and pan axes can be seen.

brushed motors which drive the eyes with toothed belts (see Fig. 9). The belts can be tensioned by means of apposite tensioning guides which are included in the mechanism. Besides the video camera and the video processing boards the head also contains the following elements:

- an XSense MTx inertial sensor, which measures the three components of linear accelerations and of angular velocities;
- a PC104 which is used for high level motor control (see Sec. 4.1);
- two small omnidirectional microphones, for auditory input;
- a MCP and two MC4 boards (see Sec. 4.2) which are used to control the neck and eye motors;
- facial expression boards, which control a set of LED's that represent the facial expressions.

4. Electronics and Sensors

4.1. *PC104*

The PC104 card is used in general for the bidirectional communication of iCub with the external control station. It is based on a Intel Core 2Duo 2.16 Mhz Pentium processor and has 1 GB of RAM, and the sensors acquisition and control electronics. The data to and from the different robot parts are transferred over several CAN bus lines. As the gradual improvements and addition of sensors (see following sections) required an increase of data throughput in its latest revision the board interfaces with ten CAN bus ports.

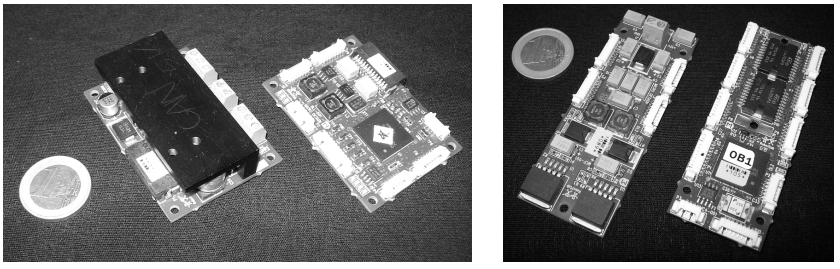

(a) (b)

Fig. 10. Motor control boards. The figure shows the custom motor control boards developed for the RobotCub project. The BLP and BLL boards for high power motor groups are shown in (a). The low power MCP and MC4 boards are shown in (b).

4.2. *Motor control boards*

The arms' brushless motors are controlled with the BLL (BrushLess Logic) and the BLP (BrushLess Power) electronic boards shown in Fig. 10(a). The BLL board processes the various signals provided by the sensors and generates the control signals that govern the motion of the motors. These signals are then passed to the BLP board which contains the actuator power drivers: the voltages applied to the three phases are controlled by the amplifiers with pulse width modulation (PWM). BLP boards can provide power up to 20 A at 48 V. Similar but smaller boards have been developed to drive small, low power DC motors. The power board and the controller board (which drives four motors independently) are conventionally called MCP and MC4 respectively. A MCP and three MC4 boards (see Fig. 10(b)) can be used to control up to 12 DC motors, delivering up to 1 A at 12 V to each motor. The electronics are placed on-board near the motor joint assemblies. Data to and from BLL and MC4 boards are exchanged through CAN bus interfaces.

4.3. *Joint position sensors*

For what concerns position sensing, each actuator unit contains three Hall effect sensors integrated in the motor stator that can be used as an incremental rotary position sensor. This provides a low resolution 48 cpr (counts per revolution) rotor position measurement which can be used for trapezoidal phase commutation. Moreover every joint angular position is sensed with an absolute 12bit angular encoder (employing the AS5045 microchip from Austria Microsystems).

In most cases there is no room to fit a position sensor in the frontal part of the motor groups since all parts move with respect to the frame. For this reason it was necessary to locate the position sensor in the rear of the motor. To do this the movement of the output link is transmitted through the motor's rotor hollow shaft with a thin shaft that carries the magnet for the sensor: this particular arrangement can be seen in Fig. 3.

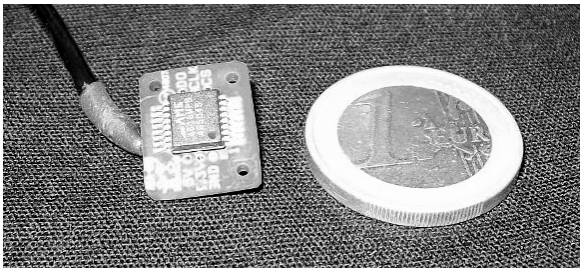

Fig. 11. AEA board. The figure shows a photograph of the 12 bit AEA encoder board.

4.4. *Six-axis force−torque sensor*

The iCub arm also comprises a six-axis force−torque sensor.[20] The sensor load cell is based on a three spoke structure machined from stainless steel Fig. 12(a). On each side of each spoke, a semi-conductor strain-gage is mounted: opposite strain gages are connected in a half Wheatstone's' bridge configuration. The sensor integrates an electronic board for the data acquisition and signal conditioning Fig. 12(b). The board samples six analog channels with an INA118 instrumentation amplifier: each input is connected to one of the six aforementioned half Wheatstone's' bridges. The analog to digital conversion is performed by an AD7685 converter on the multiplexed signals of the six channels. It is besides possible to add an offset by means of a DAC. The board also allows the installation of thermal compensation resistors that minimize the thermal drift effects of the semi-conductor strain gages (SSG). All the operations are managed with a 16bit DSP from Microchip (dsPIC30F4013) which also provides digital signal filtering and the linear transformation needed to project the signals of the strain gages to the force/torque space. The data are finally broadcast through a CAN bus interface at a frequency of 1 kHz.

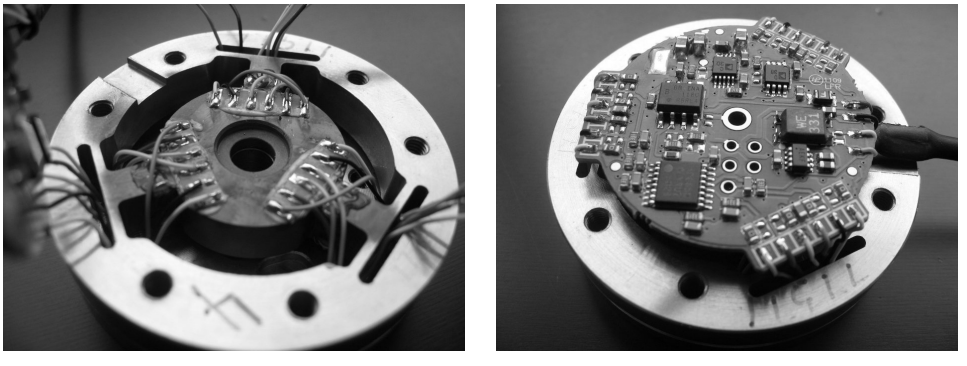

(a) (b)

Fig. 12. Six-axis force−torque sensor. The figure shows photos of the sensors' three-spoke structure (a), and the integrated electronic board (b).

4.5. *Pressure sensors for tactile feedback*

Humanoid robots are required to sustain increasingly complex forms of interaction (e.g. whole hand or whole arm grasping and manipulation,[29] etc.). In these cases the location and the characteristics of the contact cannot be exhaustively predicted or modeled in advance. Skin-like sensors and sensing methods are therefore required for processing distributed tactile information. The problem is not new and some pressure sensing technologies for humanoid robots were studied recently.[30,31]

We have equipped the hands of iCub with a distributed pressure sensing system based on capacitive technology.[32,33] This technology is based on modules which yield 12 independent measurements from 12 corresponding pressure sensing elements, called taxels in the following. The basis of each taxel is constituted by a round metal pad which is obtained on a flexible PCB. Flexible PCBs can be bent to cover generic curved surfaces and the shape can be engineered to optimize covering or curvature of the robot surface. The flexible PCBs are then covered with a thin layer of soft silicone foam, which is roughly 2.5 mm thick. This silicone layer acts as the dielectric medium of a capacitor. The foam is covered by an outer layer, which can be obtained either from conductive Lycra or from conductive silicone. This layer is connected to ground and enables the sensor to respond to objects irrespective of their electrical properties (unlike consumer electronic products based on the same technology). In addition, this layer reduces electric noise from the environment. When pressure is applied to the sensor, this conductive layer gets closer to the round pads on the PCB thereby changing their capacitance. We use this change in capacitance as an estimation of the pressure applied to the sensor surface. The taxels are connected to a capacitive to digital converter chip (AD7147 from Analog Devices), which sends the measurements over an I^2C serial bus. The data of up to 16 modules (for a total of 192 taxels) are collected by a small micro-controller board, which can then relay them to the main CPU via CAN bus.

In the first version of iCub these pressure sensors have been embedded in the palm, the fingertips and the forearm (as shown in Fig. 16(a)), to enhance the manipulation capabilities of the robot. In particular, the skin of the palm incorporates four triangular modules (see Fig. 13(a)), each of the five fingertips comprises one module (see Fig. 13(b)), and the forearm covers contain 23 modules. This arrangement results in a total of 384 independent sensitive elements per arm.

4.6. *Communication bus*

Control cards, skin sensors and force−torque sensors communicate on several 1Mbit/s CAN bus ports. The network is characterized by a star-like topology, with all branches converging on the PC104 CPU. Ten CAN sub-networks (roughly one for each body segment, and two dedicated for skin sensors) join at a central node which is constituted by the PC104, described in Sec. 4.1. This network architecture is represented in Fig. 14.

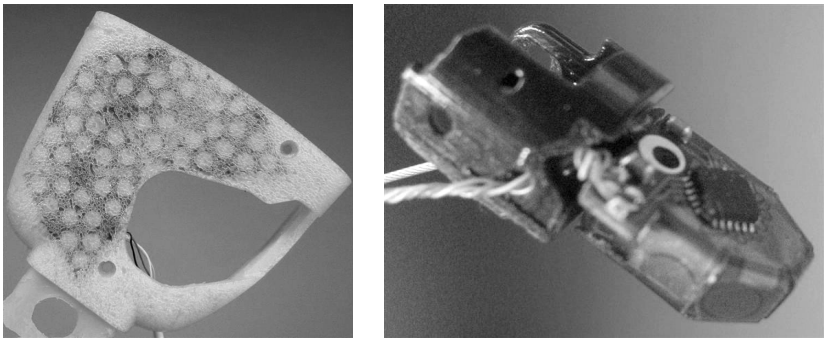

(a) (b)

Fig. 13. Tactile pressure sensors. The figure shows a photograph of the iCub palm with embedded capacitive pressure sensors (a), and a detail of the pressure sensing fingertip (b).

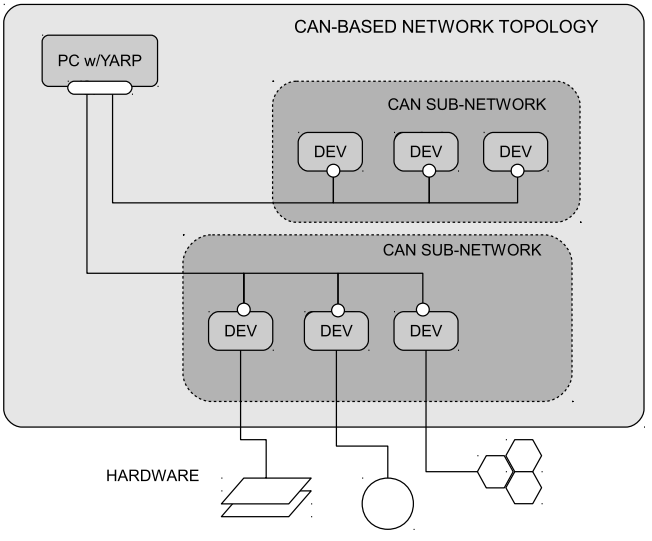

Fig. 14. iCub bus diagram. The figure shows a diagram of the current communication bus arrangement of the iCub. The control boards are called DEV int the figure.

5. iCub2

The first version of the iCub robot was developed and constructed four years ago. Since then it has intensively been used by several partners and institutions[n]: this allowed to reveal several critical aspects in its initial design. We therefore began the development of a new version of the iCub (tentatively called iCub2) which is now almost complete. The most relevant improvements are described in the following sub-sections.

[n] A comprehensive and up to date list can be found in the website *http://www.icub.org*.

5.1. *Joint torque sensing*

The requirement for the robot to interact safely and robustly with humans and its surrounding environment is particularly difficult to fulfill. To achieve this, joint torque feedback is essential. We therefore developed torque sensors for the main joints of the iCub. All the sensors are based on the piezo-resistive effect of SSG. When loads are applied the sensing elements and the SSG which are attached to them deform. This deformation is accompanied by a change in resistance which is proportional to the applied torque. The signal conditioning is preformed by microcontroller boards similar to the one described in Sec. 4.4. The sensors allow the measurement of joint torques with 16 bits of resolution at a frequency of 1 kHz. As the constraint was to maintain all the functional dimensions of the iCub unchanged, the development of the sensor for the shoulder joint (which are shown in Fig. 15(a)) was particularly complicated.[34] For the lower body instead it was possible to develop a sensor with radial, controlled deformation, spoke features, that can seamlessly be integrated in the motor groups (see Fig. 15(b)). Finite element structural simulations were employed to optimize the final sensor geometries. Although the current loop frequency is limited by the CAN bus network throughput, in the near future it will be possible to close torque feedback loops at 3 kHz by relying on a new control card design (see Sec. 5.6). The addition of joint torque sensing also required significant upgrades to the firmware and software currently used to control the robot.[35]

5.2. *Extensive tactile feedback*

Besides joint torque sensing the sense of touch is among the principal sensing modalities required to work closely and interact safely with humans and more in general with the environment. Touch can provide a reliable source of information to guide exploratory behaviors as required for example in machine learning. For this

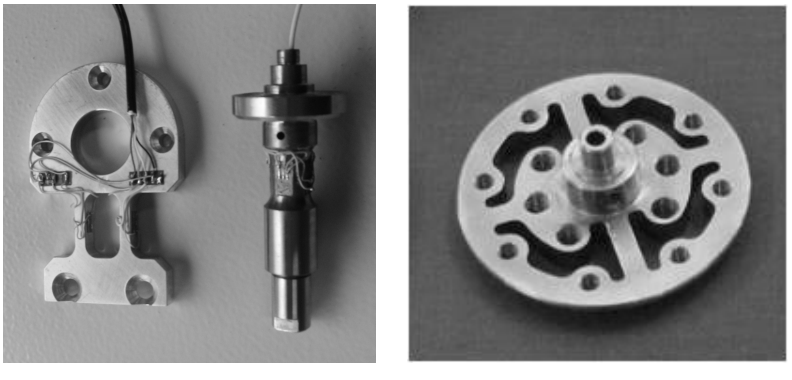

(a) (b)

Fig. 15. Joint torque sensing. The figure shows a photograph of the iCub shoulder joint torque sensors (a), and the "modular" joint torque sensor developed for the lower body (b).

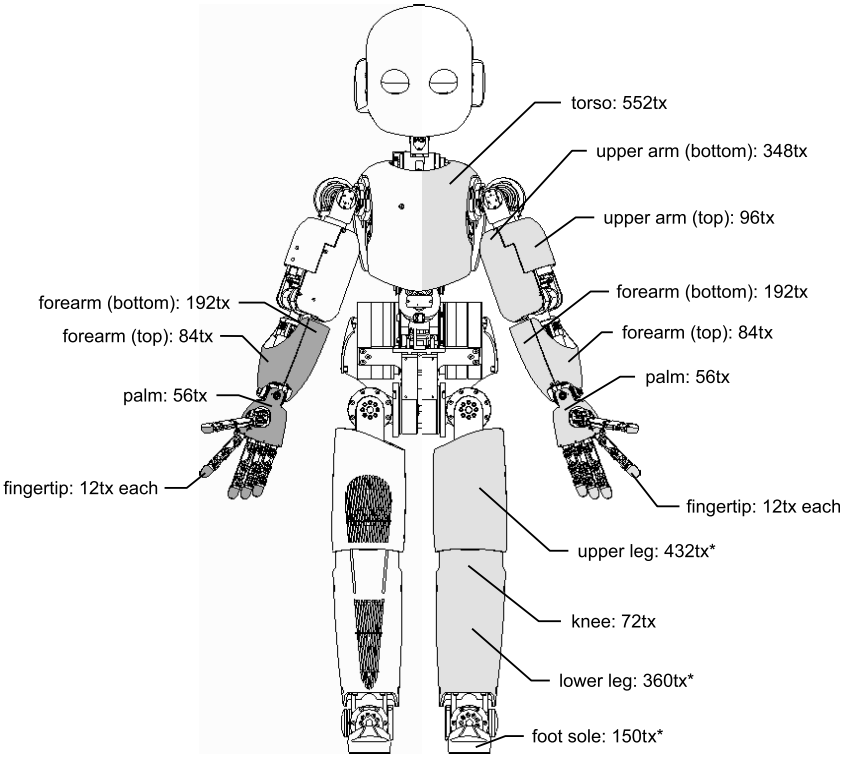

Fig. 16. Pressure sensing surfaces of the iCub. The figure shows the covers of the iCub covers with embedded pressure sensors. The surfaces colored in dark gray (a) show the pressure sensing elements of the first version of iCub. The surfaces colored in light gray (b) show the skin coverage of iCub2. The figure also indicates the number of taxels for each body segment. The numbers with the asterisk are to be intended as approximate as the design of those surfaces is currently being finalized.

reason the exterior surfaces of iCub2 have been extensively covered with the pressure sensitive elements described in Sec. 4.5. As shown in Fig. 16 the "skin" tactile sensors will be embedded in the fingertips, the palms, the forearms, the upper arm segments, the torso, the upper leg segments, the knees, the lower leg segments and the feet, for a total of approximately 4200 taxels. This, to our knowledge, makes iCub2 the humanoid robot with the highest number of pressure sensitive points. The processing of the vast amount of data streaming from these sensors will be an interesting technological challenge which is currently being addressed in the context of the RoboSKIN[o] FP7 European project.

[o] http://www.roboskin.eu/.

5.3. *Head and eyes redesign*

It was noticed that in particular operating conditions the neck motor would overheat quickly, thus indicating that they were probably under-dimensioned. A first revision of the neck mechanism, still based on the serial joint configuration, was proposed by Rodriguez.[36] The proposed solution was based on the use of harmonic drive speed reducers and four-bar linkages as key elements of the transmission. However the design was not entirely compatible with size and space constraints, and was therefore modified. This variant is based on a "parallel" actuation scheme with cable drives. The new solution is partly inspired by the design of the robot COG by Brooks *et al.*[37] which has also been employed in the construction of the MERTZ robot head.[38] As described in Sec. 3.3, epicyclic transmissions are a very effective way to reduce the driven masses and inertias. In the final design the new head assembly weights approximately 1.05 kg less than the first version of the head. With its 8 Nm peak torque on the pitch and roll axes, the new neck mechanism also allows a three-folds increase of the delivered output torque.

The eyes mechanism has also been revised. The original design was found to be critical in two senses:

- rapid eye movements were obtained with brushed DC motors which employed low reduction ratio planetary speed reducers. This introduced significant backlashes in the transmission, thus complicating the control, and in general the achievement of visual tasks.
- the tensioning of the toothed belt transmission had to be performed manually. This was problematic in terms of accuracy of the camera positioning.

The first issue is commonly solved by employing zero-backlash harmonic drive speed reducers, as done also by Asfour *et al.*[39] in the tilt joint of the ARMAR-III humanoid head. Rodriguez suggested this solution[36] as well; moreover he proposed to solve the second issue by replacing the transmission belts with low play, rigid four bar linkages. Since the elegant solution proposed by Rodriguez[36] introduced a mechanical coupling between the eyes pan and tilting motions, we preferred to maintain the current eyes mechanism configuration while improving the precision by the addition of harmonic drive gears. A CAD view of the new iCub head is shown in Fig. 17. The new neck design also features a two piece eyeball whose outer part can easily be removed to fine-tune the positioning of the cameras.

5.4. *Optical encoders*

Currently the configuration of the robot is measured by means of the magnetic joint positions sensors described in Sec. 4.3. Brushless motors are instead driven with a "standard" trapezoidal PWM profile strategy based on the feedback of three digital Hall effect sensors placed in the motor stator. These sensors provide a low resolution 48 cpr signal which causes slight vibrations when driving the motor at low speeds. To solve this issue and to implement more advanced field oriented control (FOC)

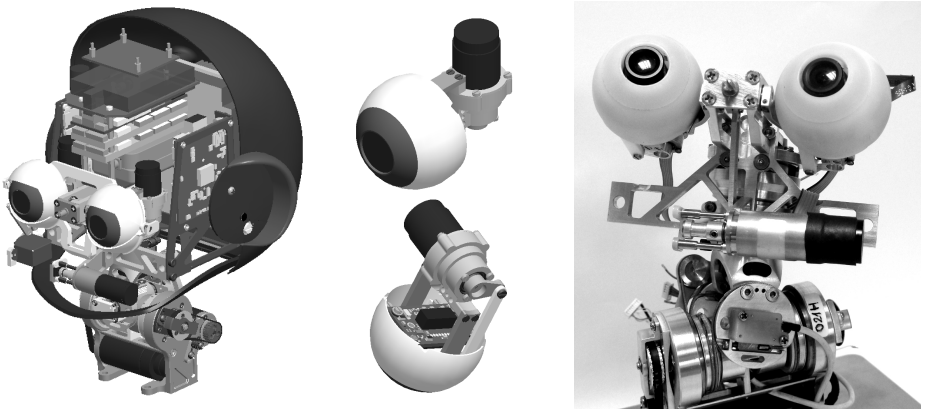

(a) (b) (c)

Fig. 17. Design revision of the iCub head. The figure shows two CAD views of the new version of the iCub head and eyes (a) and (b), and a photo of the head without the electronics (c).

strategies we developed and tested an extremely compact custom optical encoder with 8192 cpr resolution. We successfully completed the preliminary testing and are now integrating this subsystem in all the major joints of the robot.

5.5. *Control boards revision*

The control boards were improved in several ways. More in detail the first release of the BLL boards, described in Sec. 4.2, had several issues for what concerned the phases current measurement system. This system has been improved and is now capable of providing a reliable, high bandwidth, 13bit current measurement. Moreover as new sensors were added to the robot (e.g. see Sec. 5.4) the board I/O ports had to be revised, without however substantial changes. Finally the boards firmware has been thoroughly optimized with respect to its first stable release.

5.6. *Ethernet bus*

Besides the aforementioned upgrades the whole sensory motor architecture is being deeply revised. Since the current network (based CAN buses) limits the data throughput, a new Ethernet based network has been developed. The new architecture will be configured hierarchically with "mid-level" control boards called DEV in the following, supervising the operation of "low-level" boards (as represented in Fig. 18). The higher layer of the architecture will communicate on an Ethernet bus, whereas the lower level boards will employ an efficient and robust CAN transmission protocol. The solution which we are currently investigating is based on a flexible Ethernet design, where the DEVs, present two plugs for connection with a CAT5 cable. The DEVs can thus be connected either in daisy chain or in point-to-point or even in a mixture of them.

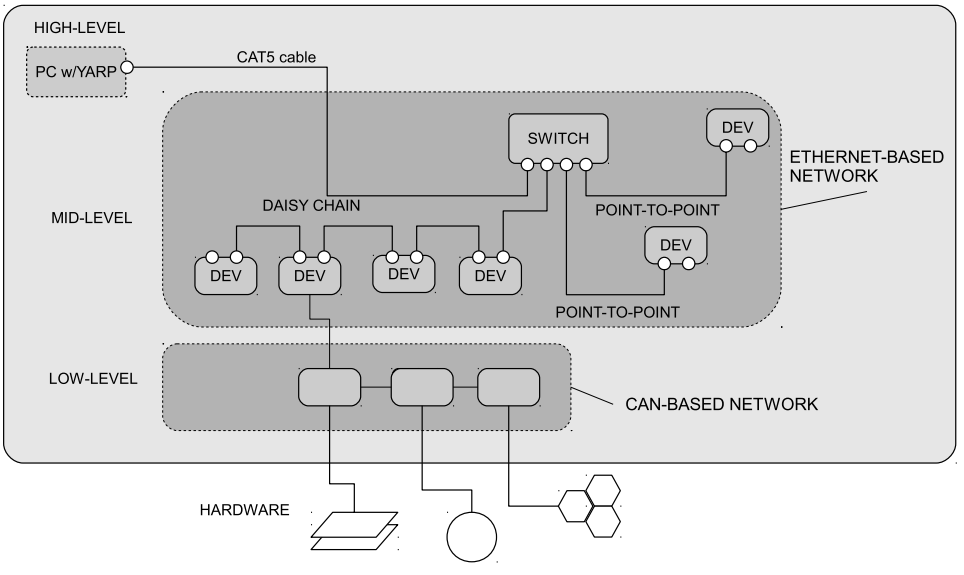

Fig. 18. Ethernet bus diagram. The figure shows a diagram of new Ethernet based network architecture.

6. Conclusions

The first part of this article presented the development of the iCub robot, which is currently being used in several robotics laboratories worldwide for research in embodied cognition.[P] In the second part the most relevant upgrades which are being integrated in the second version of the robot (namely iCub2) have been described. The robot features a combination of various technologies which make it unique; among these full joint torque feedback, extensive pressure sensing, open hardware and software can be cited as the most important. We hope that these features will make iCub2 the platform of choice for the emerging fields of artificial intelligence, motor control and developmental cognition.

Acknowledgments

This work has been supported by the European Commision RobotCub IST-FP6-004370, CHRIS IST-FP7-215805, RoboSKIN ICT-FP7-231500 and Xperience ICT-FP7-270273 projects.

We would like to thank and acknowledge the contributions to this project of Mattia Salvi, Diego Torazza, Fabrizio Larosa, Marco Accame, Claudio Lorini, Bruno Bonino, Andrea Menini, Davide Gandini, Emiliano Barbieri, Roberto Puddu, Charlie Sanguineti, Marco Pinaffo and all the people who have contributed to the

[P] For an up to date list of the demonstrations of the robot please consult the website: *http://www.youtube.com/user/robotcub.*

construction, maintenance and design of the iCub, whose help has been essential to the completion of this work.

References

1. M. Hirose and K. Ogawa, Honda humanoid robots development, *Philos. Trans. R. Soc.* **365**(1850) (2007) 11–19.
2. I. W. Park, J. Y. Kim, J. Lee and J. H. Oh, Mechanical design of the humanoid robot platform HUBO, *Adv. Rob.* **21**(11) (2007) 1305–1322.
3. T. Ishida, Y. Kuroki and J. Yamaguchi, Mechanical system of a small biped entertainment robot, in *Proc. IEEE/RSJ Int. Conf. on Intelligent Robots and Systems (IROS)*, Las Vegas, Nevada, USA, 27 October–1 November 2003, pp. 1129–1134.
4. D. Gouaillier, V. Hugel, P. Blazevic, C. Kilner, J. Monceaux, P. Lafourcade, B. Marnier, J. Serre and B. Maisonnier, Mechatronic design of NAO humanoid, in *Proc. IEEE Int. Conf. on Robotics and Automation (ICRA)*, Kobe, Japan, 12–17 May, 2009, pp. 2124–2129.
5. K. Kaneko, F. Kanehiro, M. Morisawa, K. Miura, S. Nakaoka and S. Kajita, Cybernetic human HRP-4C, in *Proc. IEEE/RAS Int. Conf. on Humanoid Robots (HUMANOIDS)*, Paris, France, 7–10 December, 2009, pp. 7–14.
6. T. Asfour, K. Regenstein, P. Azad, J. Schroder, A. Bierbaum, N. Vahrenkamp and R. Dillmann, ARMAR-III: An integrated humanoid platform for sensory-motor control, in *IEEE/RAS Int. Conf. on Humanoid Robots (HUMANOIDS)*, Geneva, Italy, 4–6 December, 2006, pp. 169–175.
7. C. Ott, O. Eiberger, W. Friedl, B. Bauml, U. Hillenbrand, C. Borst, A. Albu-Schaffer, B. Brunner, H. Hirschmuller, S. Kielhofer *et al.*, A humanoid two-arm system for dexterous manipulation, in *IEEE/RAS Int. Conf. on Humanoid Robots (HUMANOIDS)*, Nice, France, 22–26 September 2006, pp. 276–283.
8. K. Kaneko, K. Harada, F. Kanehiro, G. Miyamori and K. Akachi, Humanoid robot HRP-3, in *Proc. IEEE/RSJ Int. Conf. on Intelligent Robots and Systems (IROS)*, 2008, pp. 2471–2478.
9. C. G. Atkeson, J. G. Hale, F. Pollick, M. Riley, S. Kotosaka, S. Schaal, T. Shibata, G. Tevatia, A. Ude, S. Vijayakumar and M. Kawato, Using humanoid robots to study human behavior, *IEEE Intell. Syst.* **15**(4) (2000) 46–56.
10. A. Nagakubo, Y. Kuniyoshi and G. Cheng, The ETL-humanoid system — a high-performance full-body humanoid system for versatile real-world interaction, *Adv. Rob* **17**(2) (2003) 149–164.
11. T. Minato, Y. Yoshikawa, T. Noda, S. Ikemoto, H. Ishiguro and M. Asada, CB^2: A child robot with biomimetic body for cognitive developmental robotics, in *IEEE/RAS Int. Conf. on Humanoid Robots (HUMANOIDS)*, Pittsburgh, PA, USA, 29 November–1 December, 2007.
12. G. Cheng, H. Sang-Ho, A. Ude, J. Morimoto, J. G. Hale, J. Hart, J. Nakanishi, D. Bentivegna, J. Hodgins, C. Atkeson, M. Mistry, S. Schaal and M. Kawato, CB: Exploring neuroscience with a humanoid research platform, *Adv. Rob.* **21**(10) (2007) 1097–1114.
13. H. Bruyninckx, P. Soetens and B. Koninckx, The real-time motion control core of the Orocos project, in *Proc. IEEE Int. Conf. on Robotics and Automation (ICRA)*, Taipei, Taiwan, 14–19 September, 2003, pp. 2766–2771.
14. M. Quigley, B. Gerkey, K. Conley, J. Faust, T. Foote, J. Leibs, E. Berger, R. Wheeler and A. Y. Ng, ROS: An open-source robot operating system, in *Open-Source Software Workshop at the Int. Conf. on Robotics and Automation (ICRA)*, Kobe, Japan, 12–17 May, 2009.

15. F. Yamasaki, T. Matsui, T. Miyashita and H. Kitano, Pino the humanoid: A basic architecture, *RoboCup 2000: Robot Soccer World Cup IV*, 2001, pp. 269−278.
16. G. Metta, G. Sandini, D. Vernon, D. Caldwell, N. Tsagarakis, R. Beira, J. S. Victor, A. Ijspeert, L. Righetti, G. Cappiello, G. Stellin and F. Becchi, The robotcub project: An open framework for research in embodied cognition, in *Proc. IEEE/RAS Int. Conf. on Humanoid Robots (HUMANOIDS)*, Santa Monica, CA, USA, 10−12 November, 2004, pp. 13−32.
17. P. Fitzpatrick, G. Metta and L. Natale, Towards long-lived robot genes, *Rob. Autom. Syst.* **56** (2008) 29−45.
18. G. Metta, D. Vernon and G. Sandini, Deliverable 8.1. Initial specification of the iCub open system, 2004. Available at: http://www.robotcub.org/index.php/robotcub/content/download/614/2215/file/D8.1.pdf.
19. A. R. Tilley, *The Measure of Man & Woman: Human Factors in Design* (Wiley Interscience, 2002).
20. N. G. Tsagarakis, G. Metta, G. Sandini, D. Vernon, R. Beira, F. Becchi, L. Righetti, J. Santos-Victor, A. J. Ijspeert, M. C. Carrozza and D. G. Caldwell, iCub: the design and realization of an open humanoid platform for cognitive and neuroscience research, *Adv. Rob.* **21**(10) (2007) 1151−1175.
21. J. M. Hollerbach, I. W. Hunter and J. Ballantyne, *A Comparative Analysis of Actuator Technologies for Robotics* (MIT Press, Cambridge, MA, USA, 1992), pp. 299−342.
22. P. Dario, Deliverable 7.2, Analysis and pre-selection of the sensor and actuator technologies, 2004. Available at: http://www.robot-cub.com/index.php/robotcub/private/deliverables/deliverable_7_2_pdf.
23. J. K. Salisbury, W. T. Townsend, D. M. DiPietro and B. S. Eberman, Compact cable transmission with cable differential, Patent, Feb 1991. US 4 903 536.
24. W. T. Townsend, The effect of transmission design on force-controlled manipulator performance, PhD thesis, Massachusetts Institue of Technology, 1988.
25. W. T. Townsend and J. K. Salisury, Mechanical design for whole-arm manipulation, in *Robots and Biological Systems: Towards a New Bionics?* eds. P. Dario, G. Sandini and P. Aebischer (Springer, 1993), pp. 153−164.
26. L.-W. Tsai, *Robot Analysis* (Wiley interscience, 1999).
27. A. Parmiggiani, Torque control: A study on the iCub humanoid robot, PhD thesis, Univversitá degli Studi di Genova, (2010).
28. A. Schmitz, U. Pattacini, F. Nori, L. Natale, G. Metta and G. Sandini, in *IEEE/RAS Int. Conf. on Humanoid Robots (HUMANOIDS)*, Nashville, TN, USA, 6−9 December, 2010, pp. 186−191.
29. Y. Ohmura and Y. Kuniyoshi, Humanoid robot which can lift a 30 kg box by whole body contact and tactile feedback, in *Proc. IEEE/RSJ Int. Conf. on Intelligent Robots and Systems (IROS)*, San Diego, CA, USA, 29 October−2 November, 2007.
30. O. Kerpa, K. Weiss and H. Worn, Development of a flexible tactile sensor system for a humanoid robot, in *Proc. IEEE/RSJ Int. Conf. on Intelligent Robots and Systems (IROS)*, Vol. 1, Las Vegas, Nevada, USA, 27 October−1 November, 2003.
31. Y. Ohmura, Y. Kuniyoshi and A. Nagakubo, Conformable and scalable tactile sensor skin for curved surfaces, in *Proc. IEEE Int. Conf. on Robotics and Automation (ICRA)*, Orlando, FL, USA, 15−19 May, 2006, pp. 1348−1353.
32. G. Cannata, M. Maggiali, G. Metta and G. Sandini, An embedded artificial skin for humanoid robots, in *IEEE Int. Conf. on Multisensor Fusion and Integration for Intelligent Systems*, Seoul, South Korea, 20−23 August, 2008, pp. 434−438.
33. A. Schmitz, M. Maggiali, M. Randazzo, L. Natale and G. Metta, A arototype fingertip with high spatial resolution pressure sensing for the robot iCub, in *IEEE/RAS Int. Conf.*

on Humanoid Robots (HUMANOIDS), Daejeon, South Korea, 1–3 December, 2008, pp. 423–428.
34. A. Parmiggiani, M. Randazzo, L. Natale, G. Metta and G. Sandini, Joint torque sensing for the upper-body of the icub humanoid robot, in *Proc. IEEE/RAS Int. Conf. on Humanoid Robots (HUMANOIDS)*, Paris, France, December 7-10 2009, pp. 15–20.
35. G. Metta, P. Fitzpatrick and L. Natale, Yarp: Yet another robot platform, *Int. J. Adv. Rob. Syst.* **3**(1) (2006) 43–48.
36. N. E. N. Rodrguez, Design issue of a new iCub head sub-system, *Rob. Comput. Integr. Manuf.* **26**(2) (2010) 119–129.
37. R. A. Brooks, C. Breazeal, M. Marjanovic, B. Scassellati and M. Williamson, The cog project: Building a humanoid robot, in *Computation for Metaphors, Analogy and Agents*, Lecture Notes in Artificial Intelligence 1562 (Springer, New York, 1999), pp. 52–87.
38. L. Aryananda and J. Weber, Mertz: A quest for a robust and scalable active vision humanoid head robot, in *IEEE/RAS Int. Conf. on Humanoid Robots (HUMANOIDS)*, Santa Monica, CA, USA, 10–12 November, 2004, pp. 513–532.
39. T. Asfour, K. Welke, P. Azad, A. Ude and R. Dillmann, The Karlsruhe humanoid head, in *IEEE/RAS Int. Conf. on Humanoid Robots (HUMANOIDS)*, Daejeon, South Korea, 1–3 December, 2008, pp. 447–453.